Stress-Strain Characteristics of Soil/Reinforced Soil and Their Modelling

Swami Saran*, Zeid Thabet Youssef† and N.M. Bhandari‡

Introduction

In finite element analysis, using discrete model of representation of reinforced soil system, the friction characteristics between the soil mass and a finite length of reinforcement can be modeled by introducing an interface element of zero thickness (Goodman, et al., 1968) or thin layer elements of finite thickness (Sharma and Desai, 1992).

Several non-linear elastic models, such as bilinear model (Chiristian and Desai, 1977), K-G model (Naylor and Pande, 1981), hyperbolic model (Konder, 1963 and Duncan and Chang, 1970) and Spline function model (Desai, 1971) are available; however all models suffer from being either in accurate or from its complexity involved in the evaluation of material constants. Therefore, attempt has been made to obtain a suitable mathematical model for soil and reinforced soil as composite material in a polynomial form, which can be conveniently incorporated in the finite element algorithm. This model is simple and it represents the actual behaviour to any desired degree of accuracy by simply varying the polynomial order.

With the above objective, a systematic investigation has been carried out to determine the physical properties of the soil used, its stress-strain characteristics and stress-strain characteristics of the reinforced soil as a composite material.

*   Emeritus Fellow, Department of Civil Engineering, Indian Institute of Technology Roorkee, Roorkee – 247 667 (UA) India.

†   Assistant Professor, Department of Civil Engineering, College of Engineering, University of Aden, ADEN, Republic of Yemen.

‡   Professor, Department of Civil Engineering, Indian Institute of Technology Roorkee, Roorkee – 247 667 (UA) India.

TABLE 1 : Physical Properties of Amanatgarh Sand

S. No.	Property	Value
1	Soil type	SP (as per IS-1498-1970)
2	Effective size (D_{10})	0.19 mm
3	Uniformity coefficient (C_u)	1.30
4	Coefficient of curvature (C_c)	1.04
5	Mean specific gravity	2.65
6	Minimum void ratio	0.533
7	Maximum void ratio	0.922

On the basis of experimental data, mathematical models have been developed for soil as well as for the composite materials. These mathematical models specify the stress-strain relationships that can be conveniently adopted for non-linear finite element analysis of system involving both soil and reinforced soil composite.

Soil Used

The soil used was dry Amanatgarh sand. The physical properties of sand as determined in the laboratory according to Indian Standard Code IS:2720 (Part XIV-1968) are given in Table 1.

Types of Reinforcement

Geogrid (Netlon-CE 121) and geotextiles (Bombay Dying – PD380) were used to reinforce the sand for performing triaxial tests. The properties of these materials as given by the manufacturer are given in Table 2.
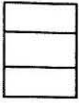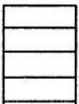
Stress-Strain Characteristics of Soil and Reinforced Soil

To obtain the stress-strain characteristics of unreinforced and reinforced sand, consolidated drained triaxial tests were performed on Amanatgarh sand at two relative densities of 50% and 80%. Extensive triaxial tests were also

TABLE 2 : Properties of Reinforcement Materials

Geogrid CE-121			Geotextile – PD 380			
Maximum load (kN/m)	Mesh apparatus size (mm)	Mesh thickness (mm)	Breaking Strength (kg), 5 × 20 cm, IS-1969-1963		Pore Size in micron	
7.68	8 × 6	3.3	247.7	182.0	25.0	69

TABLE 3 : Details of Triaxial Tests on Reinforced Soil

S.No	No. of Tests	Type of Reinforcement	No. of Layers	Relative Density	Confining Pressure (kPa)	Spacing
1	5	Geogrid	2	50%		
2	5	Geogrid	2	80%	100, 150,	
3	5	Geotextile	2	50%	200,	
4	5	Geotextile	2	80%	300, 400	
5	5	Geogrid	3	50%		
6	5	Geogrid	3	80%	100, 150,	
7	5	Geotextile	3	50%	200,	
8	5	Geotextile	3	80%	300, 400	
9	5	Geogrid	4	50%		
10	5	Geogrid	4	80%	100, 150,	
11	5	Geotextile	4	50%	200,	
12	5	Geotextile	4	80%	300, 400	

performed on samples of sand with same relative densities but reinforced with varying numbers of layers at different spacing, using two types of soil reinforcement, geogrid and geotextile. The details of tests performed are given in Table 3. At each density, five triaxial tests were performed for 100, 150, 200, 300 and 400 kPa confining pressures. Each test was conducted on a soil sample of 38.1 mm diameter and 76.2 mm height keeping a constant strain rate of 15 mm/hr. In all 70 tests were performed. All tests were performed by using "GDS", Geotechnical Digital System, to achieve better control and accuracy in the test results. Typical deviator stress versus axial strain and Poisson's ratio versus axial strain curves for sand of 50% relative density and reinforced sand of same relative density reinforced with 3-layers of geogrid are provided in Figs.1 through 4 respectively. Similar curves were obtained for all the 70 tests (Youssef, 1996).

Mathematical Modelling of Soil and Reinforced Soil Composite

A regression analysis has been carried out on triaxial test data of soil and reinforced soil for each value of confining pressure and a fifth degree polynomial has been found to best fit the experimental data of all tests. The general form of the stress-strain relationship may be expressed as:

$$
\left[\frac{(\sigma_1 - \sigma_3)}{(\sigma_1 - \sigma_3)_U}\right] = A_0 + A_1\left[\frac{\varepsilon_1}{\varepsilon_{1U}}\right] + A_2\left[\frac{\varepsilon_1}{\varepsilon_{1U}}\right]^2
$$

$$
+ A_3\left[\frac{\varepsilon_1}{\varepsilon_{1U}}\right]^3 + A_4\left[\frac{\varepsilon_1}{\varepsilon_{1U}}\right]^4 + A_5\left[\frac{\varepsilon_1}{\varepsilon_{1U}}\right]^5 \tag{1}
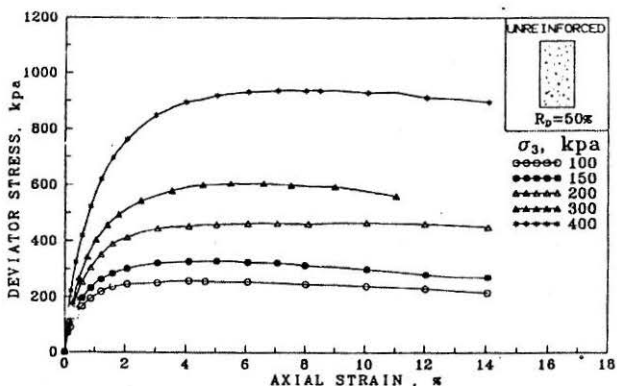$$

FIGURE 1 : Axial Strain Vs. Deviator Stress of Loose Sand (R_D = 50%)
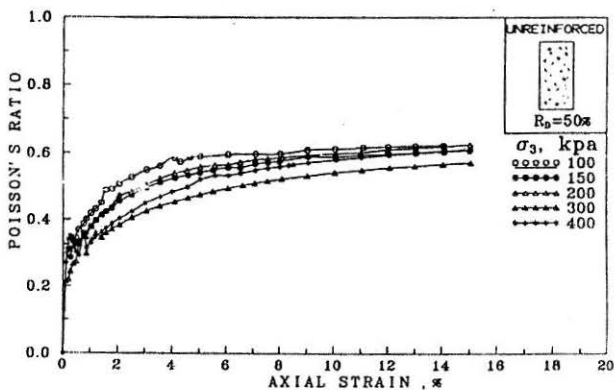

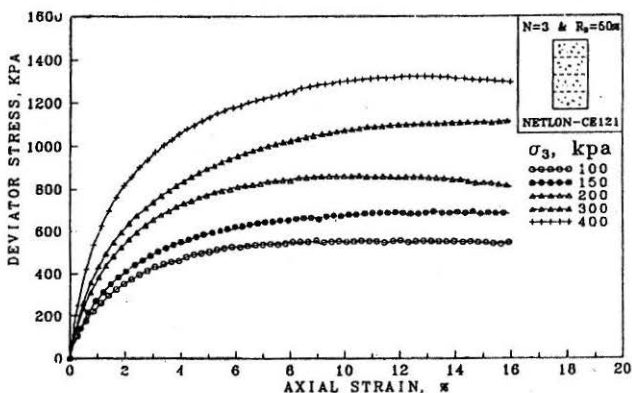FIGURE 2 : Axial Strain Vs. Poisson's Ratio of Loose Sand (R_D = 50%)

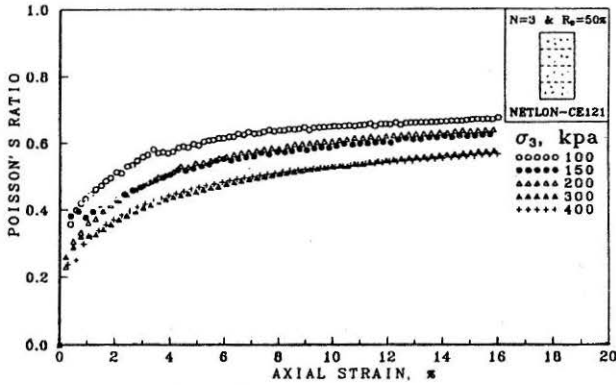FIGURE 3 : Axial Strain Vs. Deviator Stress of Loose Sand Reinforced with
3–Layers of Geogrid

FIGURE 4 : Axial Strain Vs. Poisson's Ratio of Loose Sand Reinforced with 3–Layers of Geogrid

where $(\sigma_1 - \sigma_3)$ = Deviator stress

ε_1 = Axial strain corresponding to deviator stress $(\sigma_1 - \sigma_3)$

$(\sigma_1 - \sigma_3)_U$ = Ultimate value of deviator stress

ε_{1U} = Axial strain corresponding to ultimate deviator stress $(\sigma_1 - \sigma_3)_U$

$A_0, A_1, \ldots A_5$ = Polynomial coefficients.

Typical plots showing comparison between the test results and the proposed mathematical model for unreinforced and reinforced sand are shown
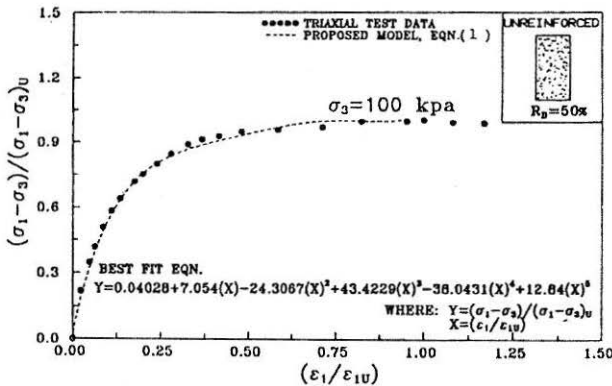

FIGURE 5 : Triaxial Tests Data and Their Best-fit for Loose Sand (R_D = 50%) for Confining Pressure = 100kPa
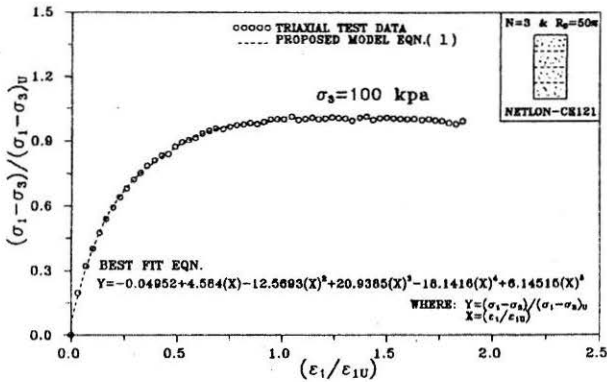
FIGURE 6 : Triaxial Tests Data and Their Best-fit for Loose Sand Reinforced with 3–Layers of Geogrid for Confining Pressure = 100kPa

in Figs.5 and 6 respectively. The best-fit equation and the best-fit curve are also given in these figures. Similar plots were obtained for other confining pressures and cases.

The values of $(\sigma_1 - \sigma_3)_U$ and ε_{1U} are determined experimentally from triaxial tests for each value of confining pressure, σ_3. Independent linear relationships have been obtained between $(\sigma_1 - \sigma_3)_U$ and σ_3, and ε_{1U} and σ_3 as shown in Figs.7 and 8 for a relative density of 50% and in Figs.9 and 10 for same relative density reinforced with three layers of geogrid. Therefore the general form of $(\sigma_1 - \sigma_3)_U$ and ε_{1U} can be written as:
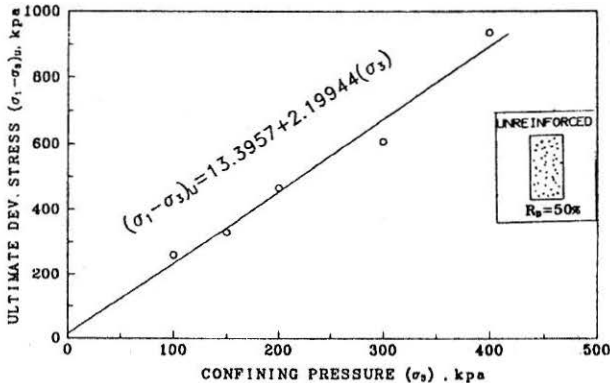

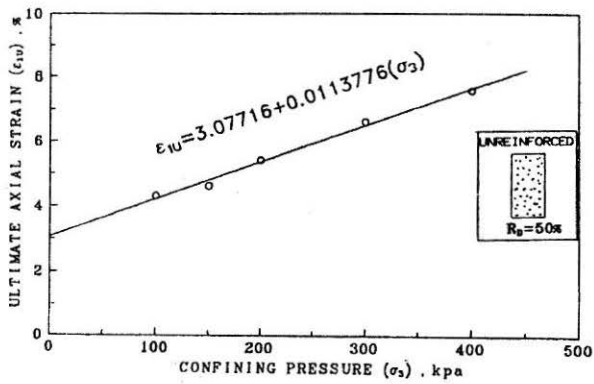**FIGURE 7 : Confining Pressure Vs. Ultimate Deviator Stress of Loose Sand (R_D = 50%)**

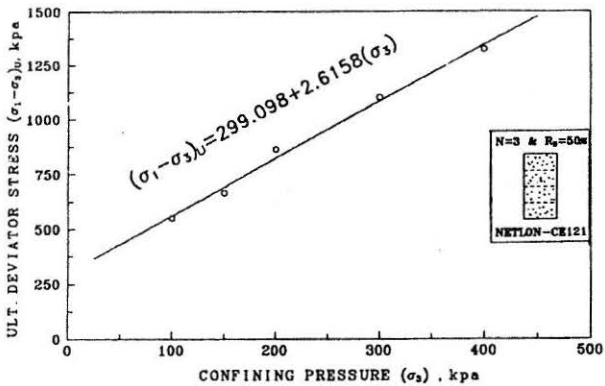FIGURE 8 : Confining Pressure Vs. Axial Strain at Ultimate Deviator Stress of Loose Sand (R_D = 50%)

FIGURE 9 : Confining Pressure Vs. Ultimate Deviator Stress of Loose Sand Reinforced with 3–Layers of Geogrid
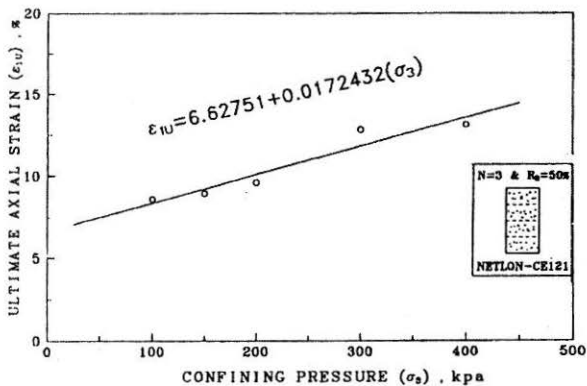

FIGURE 10 : Confining Pressure Vs. Ultimate Axial Strain of Loose Sand Reinforced with 3–Layers of Geogrid

$$(\sigma_1 - \sigma_3)_U = B_0 + B_1(\sigma_3) \tag{2}$$

$$\varepsilon_{1U} = C_0 + C_1(\sigma_3) \tag{3}$$

The values of B_0, B_1, C_0 and C_1, which are the constants of the linear equations, have been obtained from the above test results.

A_0, A_1, A_2, A_3, A_4 and A_5 are determined by regression analysis using the triaxial tests data for each values of confining pressure. Then a linear best-fit curve has been obtained for each coefficient as a function of confining pressure as shown in Figs.11 and 12 for both unreinforced and reinforced sand of 50% relative density respectively.
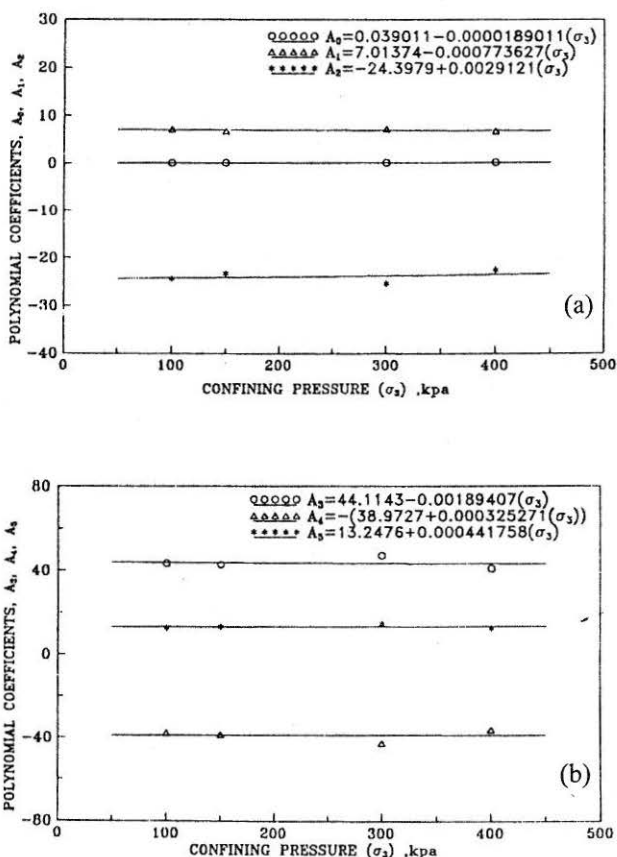

FIGURE 11 : Fifth Degree Polynomial Coefficients Vs. Confining Pressure for Loose Sand (R_D = 50%). (a) For A_0, A_1 and A_2; (b) For A_3, A_4 and A_5
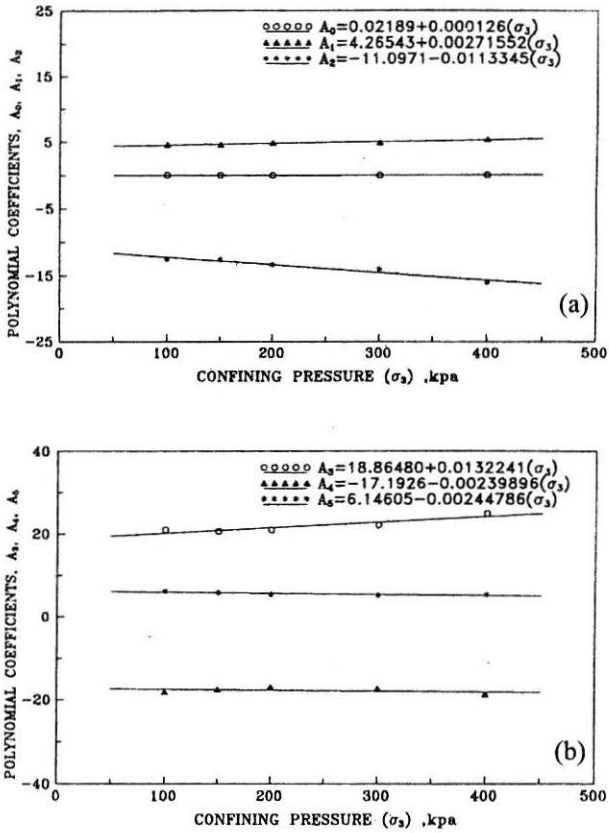
FIGURE 12 : Fifth Degree Polynomial Coefficients Vs. Confining Pressure for Loose Sand Reinforced with 3–Layers of Geogrid. (a) For A_0, A_1 and A_2; (b) For A_3, A_4 and A_5

The general form of best-fit equations for the six polynomial constants can be written as:

$$A_0 = d_0 + d_1(\sigma_3)$$
$$A_1 = d_2 + d_3(\sigma_3)$$
$$A_2 = d_4 + d_5(\sigma_3)$$
$$A_3 = d_6 + d_7(\sigma_3)$$
$$A_4 = d_8 + d_9(\sigma_3)$$
$$A_5 = d_{10} + d_{11}(\sigma_3)$$

(4)

The deviator stress-axial strain curves represented by Eqn.1 for each value of confining pressure are plotted in Figs.13 and 14 together with the triaxial test results for unreinforced and reinforced sand of 50% relative density respectively. The plots show that the proposed model represented by Eqn.1 predicts the stress-strain characteristics of sand reasonably well and is in good agreement with the experimental data. At high confining pressures, there is little difference (less than 7%). Similar trends were observed for the sand placed at relation density of 80%.

At any stress or strain level the tangent modulus of elasticity, E_T for sand can be calculated easily by differentiating Eqn.(1), so that:

$$E_T = \frac{d(\sigma_1-\sigma_3)}{d\varepsilon_1} = A_1\left[\frac{(\sigma_1-\sigma_3)_U}{\varepsilon_{1U}}\right]+2A_2\left[\frac{(\sigma_1-\sigma_3)_U}{\varepsilon_{1U}}\right]\left\{\frac{\varepsilon_1}{\varepsilon_{1U}}\right\}$$

$$+3A_3\left[\frac{(\sigma_1-\sigma_3)_U}{\varepsilon_{1U}}\right]\left\{\frac{\varepsilon_1}{\varepsilon_{1U}}\right\}^2+4A_4\left[\frac{(\sigma_1-\sigma_3)_U}{\varepsilon_{1U}}\right]\left\{\frac{\varepsilon_1}{\varepsilon_{1U}}\right\}^3$$

$$+5A_5\left[\frac{(\sigma_1-\sigma_3)_U}{\varepsilon_{1U}}\right]\left\{\frac{\varepsilon_1}{\varepsilon_{1U}}\right\}^4$$

$$E_T = \left[\frac{(\sigma_1-\sigma_3)_U}{\varepsilon_{1U}}\right]\left[A_1+2A_2\left\{\frac{\varepsilon_1}{\varepsilon_{1U}}\right\}+3A_3\left\{\frac{\varepsilon_1}{\varepsilon_{1U}}\right\}^2+4A_4\left\{\frac{\varepsilon_1}{\varepsilon_{1U}}\right\}^3+5A_5\left\{\frac{\varepsilon_1}{\varepsilon_{1U}}\right\}^4\right]$$
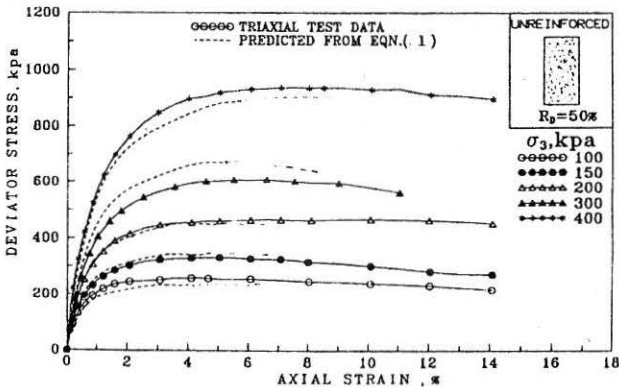
$$\ldots (5)$$

FIGURE 13 : Triaxial Tests Data and Their Predicted Values from Polynomial Eqn.1 for Loose Sand (R_D = 50%)
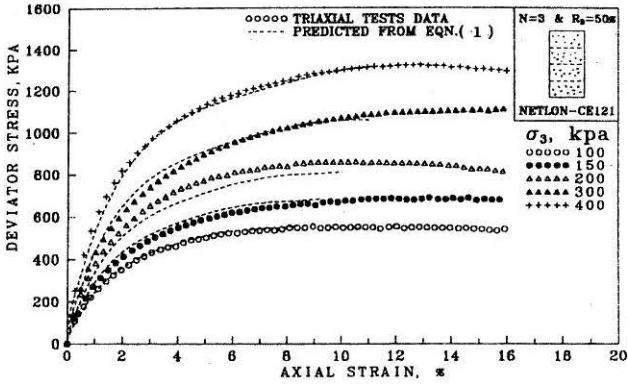
FIGURE 14 : Triaxial Test Data and Their Predicted Values from
Polynomial Eqn.1 for Loose Sand Reinforced With 3 Layers of
Geogrid

In non-linear finite element analysis, the stiffness of each soil element
is calculated based upon the proposed model (Eqn.1) which clearly defines
the non-linearity of the soil, and the tangent modulus of elasticity at any
desired stress level at each sampling Gaussian point could be computed from
Eqn.5. These element stiffness matrices are assembled suitably to give a
global stiffness matrix, which describes the static equilibrium of the structure.

Failure Criterion and Stiffness Degradation

For each load increment, the stress vectors at each Gaussian point of
a finite element are known. These values are then checked against the failure
criteria of the material to determine whether the material at that point has
failed or not. The failure criteria defines the stress or strain states at which
the material can no longer maintain its load carrying capacity. The proposed
failure criteria in the present study are:

1.   When one of the principal stresses is tensile and/or when one or both
     of the principal strains are tensile.

2.   If major principal strain $\geq \varepsilon_{1U}$

3.   If major principal stress $\geq (\sigma_1 - \sigma_3)_U$

If any one of the above conditions is satisfied at any gaussian point,
the material at that particular point is assumed to be failed. The E_T value
then drops to zero. However, for the numerical stability of the analysis E_T
is assigned a value of 0.001.

Poisson's Ratio of Soil and Reinforced Soil

The Poisson's ratio - axial strain relationship obtained from triaxial tests are shown in Figs.2 and 4 for unreinforced and reinforced sand of 50% relative densities respectively. It is evident from these figures that the Poisson's ratio varies non-linearly with the axial strain. Therefore, the non-linearity of Poisson's ratio can be modelled mathematically using a polynomial form for each value of confining pressure. Considering the small variation (less than 11.0%) in the value of Poisson's ratio with confining pressure, average values of Poisson's ratio were obtained. A best-fit polynomial of the fourth degree was found to correlate the average values of Poisson's ratio and axial strain. Thus, the general equation for Poisson's ratio can be written as:

$$\nu_i = p_0 + p_1\{\varepsilon_i\} + p_2\{\varepsilon_i\}^2 + p_3\{\varepsilon_i\}^3 + p_4\{\varepsilon_i\}^4 \tag{6}$$

where ν_i is the instantaneous Poisson's ratio at axial strain ε_i. p_0, p_1, p_2, p_3 and p_4 are the fourth degree polynomial coefficients and ε_1 is the axial strain.

The correlation of the proposed mathematical model with the test results of the Poisson's ratio for both unreinforced and reinforced sand of 50% relative density are shown in Figs.15 and 16 respectively.

Test Example

For the purpose of validation of the proposed non-linear modeling of the soil, experimental and theoretical investigations were carried out on strip footing-soil system.
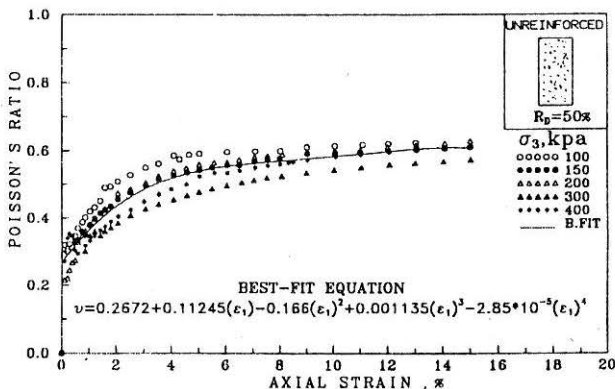

BEST−FIT EQUATION
$\nu = 0.2672 + 0.11245(\varepsilon_1) - 0.166(\varepsilon_1)^2 + 0.001135(\varepsilon_1)^3 - 2.85 \cdot 10^{-5}(\varepsilon_1)^4$

FIGURE 15 : Axial Strain Vs. Poisson's Ratio of Loose Sand ($R_D = 50\%$) and Their Best-fit
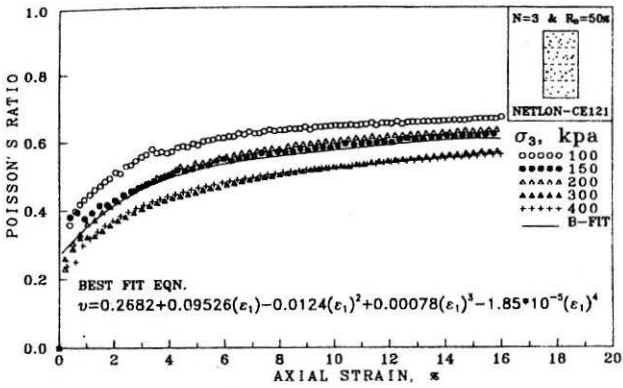
FIGURE 16 : Axial Strain Vs. Poisson's Ratio of Loose Sand Reinforced with 3 Layers of Geogrid and Their Best-fit

Two model tests on mild steel strip footing resting on dry Amanatgarh sand of 50% and 80% relative densities were performed. The size of the footing was 860 mm × 150 mm with 6.0 mm thickness. These tests were performed in a tank of 2000 mm × 870 mm of 1000 mm height fabricated out of mild steel. The pressure-settlement curve of each model was obtained and the same used for the comparison with the theoretically predicted values.
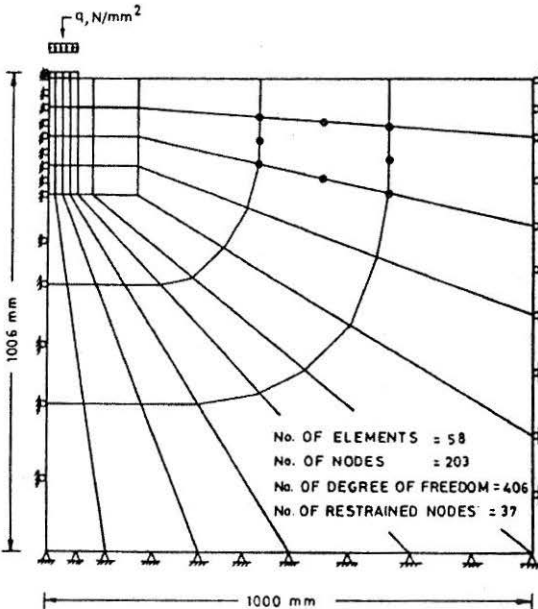

FIGURE 17 : Finite Element Idealization of Strip Footing - Soil System

Non-linear finite element analysis has been carried out using displacement formulation. Incremental-iterative technique was adopted in the non-linear formulation of finite element formulation. The footing-soil system is primarily in a state of plane strain and as such as 2-D analysis has been carried out. The system has been discretized using 8-noded solid element to represent the footing and soil element. Taking the advantage of symmetry, only half of the footing-soil system has been considered for the analysis. The finite element discretization of the system with their actual dimensions, properties and boundary conditions is shown in Fig.17. The formulation takes into account the non-linearity arising out of the non-linear behaviour of soil using the proposed model for the sand used.

The predicted pressure-settlement curves for both tests along with the experimental data are plotted in Fig.18. It is evident from this figure that the predicted results are in good agreement with the experimental data. The predicted stress distributions in the soil media along the centerline of the footing-soil media are also plotted in Fig.19 along with Boussinesq's linear solution for loads of 57.0 and 114.0 kPa with reasonable agreement. The difference is attributed to the fact that one is based on elastic model while the other on non-linear model.

From these comparisons, it can be concluded that the finite element model coupled with the proposed non-linear model of soil work well in the analysis.

Conclusions

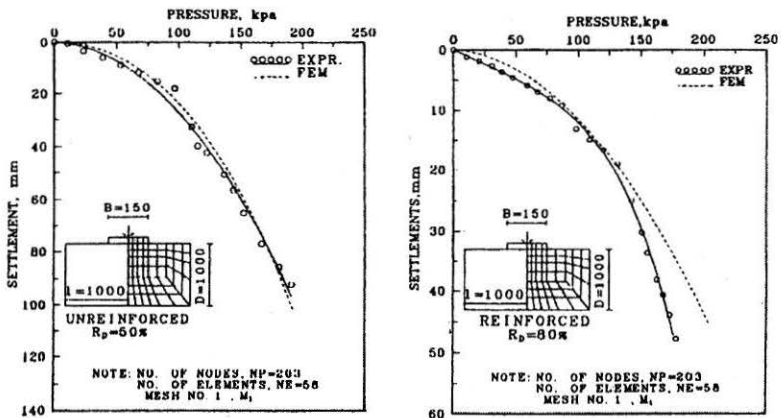In the present study, the results of triaxial tests on unreinforced and

FIGURE 18 : Pressure - Settlement Curves of Foundation for
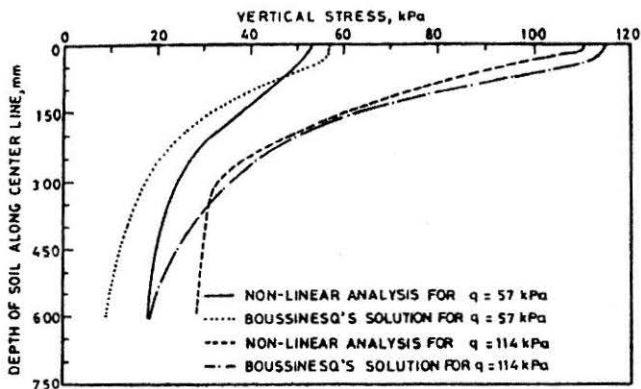(a) R_D = 50%; (b) R_D = 80%

FIGURE 19 : **Vertical Stress Distribution in the Loose Sand (R_D = 50%) at the Centre Line of the Footing**

reinforced samples of sand were obtained. On the basis of these test results, the non-linear characteristics of soil and reinforced soil composite have been defined and modeled suitably.

Similarly, the Poisson's ratio for both soil and reinforced soil system was also modeled that can be easily used in the finite element analysis. The Poisson's ratio has been found almost independent of the confining pressure.

The proposed model can be utilized in the non-linear finite element analysis of soil-structure interaction problems as has been demonstrated with an strip footing-soil system.

References

CHRISTIAN, J.T. and DESAI, C.S. (1977) : "Constitutive Laws for Geologic Media", *Numerical Methods in Geotech. Engg.* (Edited by C.D. Desai, and J.T. Christian), McGraw Hill Co., New York., Vol.1, pp.65-115.

DESAI, C.S. (1971) : "Analysis Using Spline Function", *J. SMFE Div.*, ASCE, Vol.97, No.SM10, pp.1461-1480.

DUNCAN, J.M. and CHANG, C.Y. (1970) : "Non-linear Analysis of Stress and Strain in Soils", *J. SMFE Div.*, ASCE, Vol.96, No.SM5, pp.1629-1654.

GOODMAN, R.E., TAYLOR, R.L. and BREKKE, T.L. (1968), "A Model for the Mechanics of Jointed Rocks", J. SMFE, ASCE, Vol. 94, SM3, pp. 637-659.

KONDER, R.L. (1963) : "Hyperbolic Stress-Strain Response : Cohesive Soils", *Journal of the Soil Mechanics and Foundation Divisions*, ASCE, Vol.89, No.SM1, Proc. Paper 3429, pp.115-143.

NAYLOR, D.J. and PANDE, G.N. (1981) : *Finite Elements in Geotechnical Engineering*, Pineridge Press Swansea, U.K.

SHARMA, K.G. and DESAI, C.S. (1992) : "Analysis and Implementation of Thin Layer Element for Interfaces and Joints", *J. SMFE*, ASCE, Vol.118, No.12, pp.2442-2462.

YOUSSEF, ZEID THABET (1996) : "Investigations of Plane Frame-Footings-Reinforced Soil Interaction", *Ph.D. Thesis*, Submitted in Civil Engineering Department, University of Roorkee, Roorkee, India.